Bichir external gills arise via heterochronic shift that accelerates hyoid arch development

Jan Stundl[1,2], Anna Pospisilova[1], David Jandzik[1,3], Peter Fabian[1]#, Barbora Dobiasova[1]&, Martin Minarik[1]§, Brian D. Metscher[4], Vladimir Soukup[1]*, Robert Cerny[1]*

[1] Department of Zoology, Faculty of Science, Charles University in Prague, 12844 Prague, Czech Republic
[2] National Museum, Vaclavske namesti, 11579 Prague, Czech Republic
[3] Department of Zoology, Faculty of Natural Sciences, Comenius University in Bratislava, 84215 Bratislava, Slovakia
[4] Department of Theoretical Biology, University of Vienna, 1090 Vienna, Austria

Current address: Eli and Edythe Broad CIRM Center for Regenerative Medicine and Stem Cell Research, University of Southern California, CA 90033-9080, Los Angeles, USA
& Current address: The Prague zoological garden, U Trojskeho zamku 120/3, 17100 Prague, Czech Republic
§ Current address: Department of Physiology, Development and Neuroscience, University of Cambridge, CB23DY Cambridge, United Kingdom

* corresponding authors:
Vladimir Soukup, Department of Zoology, Faculty of Science, Charles University in Prague, 12844 Prague, Czech Republic
Robert Cerny, Department of Zoology, Faculty of Science, Charles University in Prague, 12844 Prague, Czech Republic

Abstract

In most vertebrates, pharyngeal arches form in a stereotypic anterior-to-posterior progression. To gain insight into the mechanisms underlying evolutionary changes in pharyngeal arch development, here we investigate embryos and larvae of bichirs. Bichirs represent the earliest diverged living group of ray-finned fishes, and possess intriguing traits otherwise typical for lobe-finned fishes such as ventral paired lungs and larval external gills. In bichir embryos, we find that the anteroposterior way of formation of cranial segments is modified by the unique acceleration of the entire hyoid arch segment, with earlier and orchestrated development of the endodermal, mesodermal, and neural crest tissues. This major heterochronic shift in the anteroposterior developmental sequence enables early appearance of the external gills that represent key breathing organs of bichir free-living embryos and early larvae. Bichirs thus stay as unique models for understanding developmental mechanisms facilitating increased breathing capacity.

1. Introduction

The vertebrate pharynx is composed of a series of repeated embryonic structures called pharyngeal arches (Graham, 2008; Grevellec and Tucker, 2010). In the majority of jawed vertebrates, the first, or mandibular arch contributes to the jaws; the second, or hyoid arch serves as the jaw support, and the more posterior branchial arches typically bear internal pharyngeal gills. Pharyngeal arches form in a highly stereotyped sequence from anterior to posterior, where the contacts between endodermal pouches and surface ectoderm physically separate the mesoderm- and neural crest-derived arch tissues (Graham and

Smith, 2001; Shone and Graham, 2014; Choe and Crump, 2015). The progressive development of the pharynx has deep deuterostome origins, as it is characteristic of both cephalochordates and hemichordates (Willey, 1891; Gillis et al., 2012; Koop et al., 2014). In vertebrates, sequential formation of pharyngeal segments represents a fundamental aspect of the metameric organization of the head and face (Piotrowski and Nusslein-Volhard, 2000; Couly et al., 2002; Choe and Crump, 2015). Any modifications of this well-established anteroposterior differentiation scheme would represent a radical alteration in development of the stereotypic chordate bauplan (Square et al., 2017).

Polypterid bichirs represent the earliest diverged living group of ray-finned (Actinopterygian) fishes (Hughes et al., 2018) and they are often referred to as the most relevant species for studying character states at the dichotomy of ray- and lobe-finned fishes (e.g., Standen et al., 2014). This places bichirs in a unique phylogenetic position among vertebrates, which can be exploited for evolutionary and developmental comparative studies (e.g., Takeuchi et al., 2009; Standen et al., 2014; Minarik et al., 2017). Adult bichirs possess several intriguing characteristics that have been associated with air-breathing during the transition from water to land, such as ventral paired lungs or spiracular openings on the head (Clack, 2007; Coates and Clack, 1991; Graham et al., 2014; Tatsumi et al., 2016). Moreover, bichirs also share several key larval features with lungfishes or amphibians, such as cranial adhesive organs, and larval external gills (Kerr, 1907; Diedhiou and Bartsch, 2009).

The external gills of bichirs represent prominent adaptive structures, and constitute major breathing organs of their free-living embryos and early larvae (Fig. 1A) (Kerr, 1907; Diedhiou and Bartsch, 2009). Strikingly, while external gills of amphibians and lungfishes derive from branchial arches as a rule (Duellman and Trueb, 1994; Witzmann, 2004; Nokhbatolfoghahai and Downie, 2008; Schoch and Witzmann, 2011), those of bichirs have historically been considered as unique hyoid arch derivatives due to their blood supply from the hyoid aortic arch (Kerr, 1907; Goodrich, 1909). Importantly, the external gills of bichir embryos represent the first cranial structures to appear, emerging before the eyes or mouth are evident (Fig. 1B) (Minarik et al., 2017).

Here, we take advantage of an exceptionally complete embryonic series of the Senegal bichir (*Polypterus senegalus*) to explore the developmental underpinnings of the early formation of their external gills and test their segmental origin. Our results reveal that bichir external gills are definitively derived from the hyoid arch and develop by orchestrated acceleration of tissues of all germ layers of the hyoid segment. Thus, in bichir embryos, the standard anteroposterior differentiation scheme of cranial segments is modified by the unique heterochronic development of the hyoid metamere, allowing early and enhanced development of their external gills.

2. Results and discussion

2.1. External gills of the Senegal bichir are developmentally associated with the hyoid segment

In order to examine the origin of bichir external gills, we first followed the morphological development of this structure from the earliest stages of embryogenesis onwards. The first sign of external gill development is a pair of outgrowths situated lateral to the closing neural folds (Fig. 1C). The hyoid origin of these outgrowths is suggested by the expression pattern of the *Hoxa2* (Fig. 1D), a selector gene characteristic of hyoid identity in other vertebrates (Rijli et al., 1993; Hunter and Prince, 2002; Baltzinger et al., 2005). Later, at early pharyngula stages, the hyoid outgrowths produce protuberant bulges situated in the pre-otic region on each side of the embryo (Fig. 1E-H), that rapidly increase in size (Fig. 1I), and finally, differentiate into many secondary branches (Fig. 1J-L). This suggests that the prominent external gills of bichir larva (Fig. 1A) initially arise from striking accelerated development of the epidermal outgrowths (Fig. 1B) that are of hyoid segmental origin (Fig. 1F).

2.2. Accelerated and predominant hyoid neural crest stream supplies bichir external gills

To gain insights into the accelerated development of the hyoid segment, we focused on the cranial neural crest that arises from the closing neural folds. Cranial neural crest cells emerge in a characteristic pattern and split into mandibular, hyoid, and branchial streams, which in most vertebrates arise in a sequential anteroposterior order of appearance. As a marker for migrating neural crest cells, we used expression of *Sox9*, a transcription factor critical for their emergence, migration, and differentiation (Cheung and Briscoe, 2003; Mori-Akiyama et al., 2003; Theveneau and Mayor, 2012). In bichir embryos, *Sox9* expression pattern reveals that the hyoid neural crest segment is developmentally advanced, as it forms concurrently with the mandibular neural crest segment (Fig. 2A). Sections through the neural folds, however, demonstrate that mandibular neural crest cells still reside within the neuroepithelium (Fig. 2B), while the hyoid neural crest cells have already emigrated from the neural folds (Fig. 2C). This premature emigration of the hyoid neural crest stream correlates with the previously observed external outgrowths of the hyoid area (Fig. 1C). Later in migration, the hyoid neural crest stream remains predominant (Fig. 2D), as it is much larger when compared to the mandibular neural crest stream (Fig. 2E, F). The hyoid neural crest stream still progresses at later stages (Fig. 2G), and as such, the majority of the mesenchyme in the early bichir head appears to arise from this source (Fig. 2H). The Sox9 immunoreactivity further shows that cells of the leading edge of the hyoid stream delaminate from the neural folds prior to the emigration of the mandibular stream (Fig. 2I), and illustrates the voluminous (Fig 2J) and extended (Fig 2K) mesenchymal production of the hyoid neural crest segment.

We directly tested whether the hyoid neural crest cell stream contributes to the external gills by performing focal CM-DiI injections into rhombomere 4 (Fig. 2L inset), the source of the prospective hyoid neural crest stream in other vertebrates (Lumsden et al., 1991; Köntges and Lumsden, 1996; Minoux and Rijli, 2010; Theveneau and Mayor, 2012). One day after neurulation, the CM-DiI-positive hyoid neural crest cells are observed all along the proximodistal axis of the external gill primordium (Fig. 2L). Two days later, they occupy the primary branches of the external gills (16/21, Fig. 2M). After hatching, the CM-DiI-positive cells populate the fully developed and functional external gills (Fig. 2N, O). Thus, our fate mapping experiment confirms that bichir external gills are, indeed, populated by the cells of the hyoid neural crest stream and, implicitly, that they represent hyoid arch derivatives.

2.3. The first cranial muscles of bichir embryos support their external gills and are of hyoid segmental origin

In vertebrates, cranial neural crest cells are the primary source of craniofacial mesenchyme, but also have a major influence on the differentiation and morphogenesis of the cranial myogenic mesoderm (Ericsson et al., 2004; Tokita and Schneider, 2009). We, therefore, hypothesized that the pattern of cranial muscle differentiation in bichir embryos may be

affected by acceleration of the hyoid neural crest segment (Fig. 2). Whole-mount antibody staining against skeletal muscle marker 12/101 revealed that the first muscles differentiate stereotypically from the post-otic somites in the trunk region, as in other vertebrates (Fig. 3A). However, within the cranial region of bichir embryos, the earliest developing muscles form within the hyoid arch and are associated with the external gills (Fig. 3B, C). This first muscle complex (*levator and depressor branchiarum*, Noda et al., 2017) is situated lateral to the otic vesicle and connects filaments of the external gills to the gill stem (Fig. 3B-D). The premature differentiation of the external gill-associated muscles is further supported by their innervation from the hyo-opercular ramus of the facial nerve, allowing voluntary movement of external gills from the earliest larval stages (Fig. 3E, F). Other cranial muscles fully differentiate only at later larval stages when the external gill muscle complex becomes supplemented by other muscles of hyoid and mandibular origins (Fig. 3G). Thus, bichir embryos display unique heterochrony in the differentiation of the hyoid over the mandibular arch mesoderm, providing muscular supports for their external gills.

2.4. Early expansion of the hyoid endoderm triggers the formation of bichir external gills

Interestingly, the accelerated development of the external gill rudiments is also reinforced by the morphogenesis of the hyoid pharyngeal segment (Fig. 4A-J). Reconstruction of the endodermal epithelium of the bichir pharynx using micro-CT imaging (Minarik et al., 2017) reveals that the pharyngeal endoderm forms two pairs of early outpocketings (Fig. 4B). Whereas the rostral pair represents the embryonic precursor of the cement glands (Fig. 4A-D, F-I) (Minarik et al., 2017), the posterior paired outpocketings constitute primordia of the external gills (Fig. 4A-D). These posterior outpocketings belong to the hyoid segment, as the first pharyngeal pouch (mandibulo-hyoid, or spiracular) is situated rostrally (Fig. 4C, D, white arrowhead) and the second pharyngeal pouch (hyoid-branchial) more caudally (Fig. 4H, black arrowhead). Transverse sections confirm that these hyoid endodermal outpocketings constitute a substantial proportion of the external gill primordium (Fig. 4E). At later stages, these outpocketings further transform into pocket-like structures (Fig. 4G, H, J) that become supplemented with mesenchymal cells of the hyoid neural crest stream (Fig. 2L-N). Thus, while ectoderm covers the entire external gill primordium, the endodermal outpocketing constitutes a considerable portion of the developing external gill (Fig. 4E).

We sought to explore a possible role of the hyoid endodermal outpocketings in controlling development and morphogenesis of the bichir external gills. Morphogenesis of the pharyngeal pouches is critically regulated by factors from many signaling pathways (Graham and Smith, 2001; Graham, 2008), among which alterations in Fibroblast growth factor (Fgf) signaling lead to defects in proper endodermal pouch development and pharyngeal segmentation (Jandzik et al., 2014; Abu-Issa et al., 2002; Crump et al., 2004; Walshe and Mason, 2003). To assess the possible role of Fgf signaling during bichir external gill development, we scored expression of the *Fgf8* ligand and the readouts of Fgf signaling activity. *Fgf8* expression is present in endodermal outpocketings and becomes confined to their lateral portions (Fig. 4-figure supplement 1). These portions of endoderm in fact constitute the outgrowing tips of the prospective external gill (Fig. 4K). Expression of *Dusp6* and *Pea3* (the Fgf signaling pathway readouts) and antibody localization for activated MAPK (marker of active Fgf signaling) are present in the external gill mesenchyme adjacent to the outgrowing endodermal tips or both in the mesenchyme and the endodermal tips (Fig. 4L-N; Fig. 4-figure supplement 2). The topographical relation of endodermal outpocketings and the direction of Fgf signaling within the external gill primordium thus suggest that the endodermal epithelium signals to the adjacent mesenchyme through Fgf signaling to regulate outgrowth of the external gill (Fig. 4O).

To test the possible role of signaling events, we treated bichir embryos with SU5402, a collective Fgf and Egf signaling inhibitor, at early neurulation and scored the phenotypes at later pharyngula stages. In contrast to control embryos displaying well-developed hyoid endodermal outpocketings and external gill primordia (18/18, Fig. 4P-Q), disrupting Fgf signaling perturbs morphogenesis of the hyoid endodermal outpocketings and leads to the

loss of the external gill primordia (14/15, Fig. 4R-S) possibly due to the loss of expression of downstream genes (Fig. 4T-U). These results support a central role of the pharyngeal endoderm in triggering early development of bichir external gills. The pharyngeal origin of the external gill primordia is surprising given that the external gills are commonly considered as outer surface structures composed of ectoderm (Takeuchi et al., 2009; Diedhiou and Bartsch, 2009). However, our finding of an endodermal component in the early formation of bichir external gills reveals an unanticipated similarity with the true, internal gills of vertebrates, which typically form as pharyngeal endodermal structures (Warga and Nüsslein-Volhard, 1999; Gillis and Tidswell, 2017). Pharyngeal morphogenesis might thus represent a central developmental component of vertebrate gill breathing organs irrespective of their actual topographic position.

3. Conclusions

The sequential formation of pharyngeal segments during embryonic development has deep deuterostome origins (Willey, 1891; Koop et al., 2014; Gillis et al., 2012) and it is well conserved among vertebrates, where all the embryonic cranial segments typically follow the sequential anteroposterior order during development (Quinlan et al., 2004; Grevellec and Tucker, 2010; Schilling, 2008; Santagati and Rijli, 2003). Bichir embryos diverge from this common scheme by the profoundly accelerated development of the second, hyoid segment, with earlier and orchestrated formation of the endodermal, mesodermal, and neural crest tissues (Fig. 5). This unique heterochronic shift in the anteroposterior sequence constitutes a developmental basis for the early appearance of external gills that represent key breathing organs of bichir free-living embryos and early larvae.

Bichir external gills significantly differ from the external gills of amphibian and lungfish larvae that characteristically supplement the post-hyoid, branchial arches (Duellman and Trueb, 1994; Witzmann, 2004; Nokhbatolfoghahai and Downie, 2008; Schoch and Witzmann, 2011). The hyoid segmental origin represents a major developmental dissimilarity and suggests an independent evolution of bichir external gills. Developmentally, bichir external gills likely correspond to opercular structures that in ray-finned fishes typically form as caudal expansions of the hyoid arch to cover the gill-bearing branchial arches, and that persist in amniotes as early embryonic opercular flaps (Richardson et al., 2012). In bichirs, the opercular flap forms directly from the base of their external gills, and it progressively expands during early larval stages while external gills become reduced (Diedhiou and Bartsch, 2009). Interestingly, the hyoid arch-derived external gills and opercular flaps are both engaged in breathing and gill ventilation in bichir larvae. Moreover, in adult bichirs, the hyoid domain also contributes to air-breathing by forming paired spiracular chamber with openings located on the dorsal surface of the skull (Graham et al., 2014). Bichirs thus seem unique across recent vertebrates in enhancing breathing capacity through the development of several structures associated with the hyoid cranial segment.

4. Materials and Methods

4.1. Embryo collection

Fish were manipulated in accordance with the institutional guidelines for the use of embryonic material and international animal welfare guidelines (Directive 2010/63/EU)**.** Senegal bichir (*Polypterus senegalus* Cuvier, 1829) embryos were obtained, reared and staged as previously described (Minarik et al., 2017; Diedhiou and Bartsch, 2009). Embryos were dechorionated manually, fixed in 4% PFA in 0.1 M PBS at 4°C overnight, and then gradually dehydrated through a series of PBS/methanol mixtures and finally stored in 100% methanol.

4.2. In situ hybridization and fate mapping

Whole-mount *in situ* hybridization with probes against *Hoxa2* (GenBank accession number: MK630352), *Sox9* (GenBank accession number: MK630350), *Fgf8* (GenBank accession number: MK630353), *Pea3* (GenBank accession number: MK630351), and *Dusp6* (GenBank accession number: MK630349) was performed as described (Minarik et al., 2017). Selected specimens were embedded in gelatine/albumin solution with glutaraldehyde, sectioned and counterstained with DAPI. Fate mapping experiments were carried out as described (Minarik et al., 2017). CM-DiI was injected into the neural fold of the prospective rhombomere 4 (Fig. 2L). To confirm correct localisation of the tracking dye, some embryos were fixed immediately after injection, sectioned, and observed under the fluorescent stereomicroscope in order to confirm proper localization of the cell tracking dye. The rest of the specimens were incubated until the desired stage and then fixed in 4% PFA in 0.1 M PBS.

4.3. Scanning electron microscopy (SEM) and MicroCT imaging

Samples for SEM were fixed in modified Karnovsky's fixative (Mitgutsch et al., 2008). For direct visualization of cranial neural crest streams, the epidermis was removed using tungsten needles as described (Cerny et al., 2004). Specimens for MicroCT analysis were treated with phosphotungstic acid following the protocol developed by Metscher (2009) and scanned with a MicroXCT (X-radia) at the Department of Theoretical Biology, University of Vienna. Images were reconstructed in XMReconstructor (X-Radia), and virtual sections were analyzed in Amira (FEI Software).

4.4. Antibody staining

Specimens for antibody staining were fixed in Dent's fixative. Muscles were labeled with 12/101 antibody (AB531892; Developmental Studies Hybridoma Bank), neural crest cells were labeled with Sox9 antibody (AB5535; Merck Millipore), basal lamina was labeled with anti-fibronectin (A0245; DAKO) and MAPK activity was assessed using anti-activated MAP kinase antibody (M8159; Sigma). Primary antibodies were detected by Alexa Fluor 488 and 594 (Invitrogen, Thermo Fisher Scientific Inc.). Visualisation of nerve fibres was performed using anti-acetylated tubulin antibody (T6793; Sigma) and EnzMet Enzyme Metallography kit (Nanoprobes).

4.5. Pharmacological treatments

For inhibition of pharyngeal outpocketing morphogenesis, embryos were treated with 50 µM SU5402 in DMSO (Sigma Aldrich) from stage 20 until stage 26. Treatments were performed in E2 medium (Brand et al., 2002). Controls were reared in E2 medium with the equivalent DMSO concentrations.

Author contributions

JS and RC conceived project and designed experiments; JS, AP, DJ, PF, BD, MM and BDM performed the experiments; JS, AP and VS analyzed the data; JS, DJ, VS and RC wrote the manuscript; all authors read and approved the final version of the manuscript.

Conflict of interest

The authors declare no competing interest.

Acknowledgments

We thank Wojta Miller and Karel Kodejs for bichir colony care; James P. Cleland, Tatjana Haitina, Dan Medeiros, Rolf Ericsson and Jana Stundlova for critical reading of earlier versions of the manuscript; Martin Kralovic for initial work on this topic, Viktoria Psutkova

and Kristyna Markova for technical assistance. This study was supported by the Charles University Grant Agency GAUK 1448514 (to J.S.), GAUK 640016 (to A.P.), GAUK 220213 and GAUK 726516 (to M.M.), the Charles University grant SVV 260434/2019 (to J.S., A.P., V.S., D.J. and R.C.), the Charles University Research Centre program No. 204069 (to V.S.), the grant of the Scientific Grant Agency of Slovak Republic VEGA 1/0415/17 and the European Union's Horizon 2020 research and innovation program under the Marie Skłodowska-Curie grant agreement No 751066 (to D.J.), and the Czech Science Foundation GACR 16-23836S (to R.C.). Computational resources were supplied by the Ministry of Education, Youth and Sports of the Czech Republic under the Projects CESNET (Project No. LM2015042) and CERIT-Scientific Cloud (Project No. LM2015085) provided within the program Projects of Large Research, Development and Innovations Infrastructures.

References

Abu-Issa R, Smyth G, Smoak I, Yamamura K, Meyers EN. 2002. Fgf8 is required for pharyngeal arch and cardiovascular development in the mouse. *Development* **129**:4613-4625.

Baltzinger M, Ori M, Pasqualetti M, Nardi I, Rijli FM. 2005. *Hoxa2* knockdown in *Xenopus* results in hyoid to mandibular homeosis. Developmental Dynamics **234**:858-867.

Brand M, Granato M, Nusslein-Volhard C. 2002. Keeping and raising zebrafish. In Zebrafish: A practical approach. (eds. C. Nusslein-Volhard and R. Dahm). Oxford University Press. p. 7–37.

Cerny R, Meulemans D, Berger J, Wilsch-Bräuninger M, Kurth T, Bronner-Fraser M, Epperlein HH. 2004. Combined intrinsic and extrinsic influences pattern cranial neural crest migration and pharyngeal arch morphogenesis in axolotl. *Developmental Biology* **266**:252-269.

Cheung M, Briscoe J. 2003. Neural crest development is regulated by the transcription factor Sox9. *Development* **130**:5681-5693.

Choe CP, Crump JG. 2015. Dynamic epithelia of the developing vertebrate face. *Current Opinion in Genetics & Development* **32**:66-72.

Clack JA. 2007. Devonian climate change, breathing and the origin of the tetrapod stem group. *Integrative and Comparative Biology* **47**:510-523.

Coates MI, Clack J. 1991. Fish-like gills and breathing in the earliest known tetrapod. *Nature* **352**:234-236.

Couly G, Creuzet S, Bennaceur S, Vincent C, Le Douarin NM. 2002. Interactions between Hox-negative cephalic neural crest cells and the foregut endoderm in patterning the facial skeleton in the vertebrate head. *Development* **129**:1061-1073.

Crump JG, Maves L, Lawson ND, Weinstein BM, Kimmel CB. 2004. An essential role for Fgfs in endodermal pouch formation influences later craniofacial skeletal patterning. *Development* **131**:5703-5716.

Diedhiou S, Bartsch P. 2009. Staging of the early development of *Polypterus* (Cladistia: Actinopterygii). In: Development of Non-Teleost Fishes. (eds Kunz-Ramsay YW, Luer CA, Kapoor BG). Enfield: Science Publishers. p. 104-109.

Duellman WE, Trueb L. 1994. Biology of Amphibians. McGraw-Hill, New York.

Ericsson R, Cerny R, Falck P, Olsson L. 2004. Role of cranial neural crest cells in visceral arch muscle positioning and morphogenesis in the Mexican axolotl, Ambystoma mexicanum. *Developmental Dynamics* **231**:237-247.

Giles S, Xu G-H, Near TJ, Friedman M. 2017. Early members of 'living fossil' lineage imply later origin of modern ray-finned fishes. *Nature* **549**:265-268.

Gillis AJ, Fritzenwanker JH, Lowe CJ. 2012. A stem-deuterostome origin of the vertebrate pharyngeal transcriptional network. *Proceedings of the Royal Society B: Biological Sciences* **279**:237-246.

Gillis JA, Tidswell ORA. 2017. The origin of vertebrate gills. *Current Biology* **27**:729-732.

Goodrich ES. 1909. Vertebrata Craniata (first fascicle: cyclostomes and fishes). In: Lankester R, ed. Treatise on zoology. Part 9. London: Adam and Charles Black.

Graham A, Smith A. 2001. Patterning the pharyngeal arches. *Bioessays* **23**:54-61.

Graham A. 2008. Deconstructing the pharyngeal metamere. *Journal of Experimental Zoology Part B: Molecular and Developmental Evolution* **310**:336-344.

Graham JB, Wegner NC, Miller LA, Jew CJ, Lai NC, Berquist RM, Frank LR, Long JA. 2014. Spiracular air breathing in polypterid fishes and its implications for aerial respiration in stem tetrapods. *Nature Communications* **5**:3022.

Grevellec AV, Tucker AS. 2010. The pharyngeal pouches and clefts: Development, evolution, structure and derivatives. *Seminars in Cell and Developmental Biology* **21**:325-332.

Hughes LC, Ortí G, Huang Y, Sun Y, Baldwin CC, Thompson AW, Arcila D, Betancur-R R, Li C, Becker L, Bellora N, Zhao X, Li X, Wang M, Fang C, Xie B, Zhou Z, Huang H, Chen S, Venkatesh B, Shi Q. 2018. Comprehensive phylogeny of ray-finned fishes (Actinopterygii) based on transcriptomatic and genomic data. *PNAS* **115**:6249-6254.

Hunter MP, Prince VE. 2002. Zebrafish hox paralogue group 2 genes function redundantly as selector genes to pattern the second pharyngeal arch. *Developmental Biology* **247**:367-389.

Jandzik D, Hawkins MB, Cattell MV, Cerny R, Square TA. Medeiros, D. M., 2014. Roles for FGF in lamprey pharyngeal pouch formation and skeletogenesis highlight ancestral functions in the vertebrate head. *Development* **141**:629-638.

Kerr JG. 1907. The development of *Polypterus senegalus* Cuvier. In: Kerr J.G., editor Budget Memorial Volume. Cambridge: Cambridge University Press.

Koop D, Chen J, Theodosiou M, Carvalho JE, Alvarez S, de Lera AR, Holland LZ, Schubert M. 2014. Roles of retinoic acid and Tbx1/10 in pharyngeal segmentation: amphioxus and the ancestral chordate condition. *EvoDevo* **5**: 36.

Köntges G, Lumsden A. 1996. Rhombencephalic neural crest segmentation is preserved throughout craniofacial ontogeny. *Development* **222**:3229-3242.

Lumsden AL, Sprawson N, Graham A. 1991. Segmental origin and migration of neural crest cells in the hindbrain region of the chick embryo. *Development* **113**:1281-1291.

Metscher BD. 2009. MicroCT for Developmental biology: A Versatile tool for high-contrast 3D imaging at histological resolutions. *Developmental Dynamics* **238**:632-640.

Minarik M, Stundl J, Fabian P, Jandzik D, Metscher BD, Psenicka M, Gela D, Osorio-Pérez A, Arias-Rodriguez L, Horácek I, Cerny R. 2017. Pre-oral gut contributes to facial structures in non-teleost fishes. *Nature* **547**:209-212.

Minoux M, Rijli FM. 2010. Molecular mechanisms of cranial neural crest cell migration and patterning in craniofacial development. *Development* **137**:2605-2621.

Mitgutsch C, Piekarski N, Olsson L, Haas A. 2008. Heterochronic shifts during early cranial neural crest cell migration in two ranid frogs. *Acta Zoologica-Stockholm* **89**:69-78.

Mori-Akiyama Y, Akiyama H, Rowitch DH, de Crombrugghe B. 2003. Sox9 is required for determination of the chondrogenic cell lineage in the cranial neural crest. *PNAS* **100**:9360-9365.

Noda M, Miyake T, Okabe M. 2017. Development of cranial muscles in the actinopterygian fish Senegal bichir, *Polypterus senegalus* Cuvier, 1829. *Journal of Morphology* **278**:450-463.

Nokhbatolfoghahai M, Downie J. 2008. The external gills of anuran amphibians: Comparative morphology and ultrastructure. *Journal of Morphology* **269**:1197-1213.

Piotrowski T, Nusslein-Volhard C. 2000. The endoderm plays an important role in patterning the segmented pharyngeal region in zebrafish (Danio rerio). *Developmental Biology* **225**:339-356.

Quinlan R, Martin P, Graham A. 2004. The role of actin cables in directing the morphogenesis of the pharyngeal pouches. *Development* **131**:593-599.

Richardson J, Shono T, Okabe M, Graham A. 2012. The presence of an embryonic opercular flap in amniotes. *Proceedings of the Royal Society B: Biological Sciences* **279**:224-229.

Rijli FM, Mark M, Lakkaraju S, Dierich A, Dollé P, Chambon P. 1993. A homeotic transformation is generated in the rostral branchial region of the head by disruption of Hoxa-2, which acts as a selector gene. *Cell* **75**:1333-1349.

Santagati F, Rijli FM. 2003. Cranial neural crest and the building of the vertebrate head. *Nature Reviews Neuroscience* **4**:806-818.

Schilling TF. 2008. Anterior-posterior patterning and segmentation of the vertebrate head. *Integrative and Comparative Biology* **48**:658-667.

Schoch RR, Witzmann F. 2011. Bystrow's Paradox - gills, fossils, and the fish-to-tetrapod transition. Acta Zoologica **92**: 251-265.

Square T, Jandzik D, Romášek M, Cerny R, Medeiros D. 2017. The origin and diversification of the developmental mechanisms that pattern the vertebrate head skeleton. *Developmental Biology* **427**:219-229.

Standen EM, Du TY, Larsson HCE. 2014. Developmental plasticity and the origin of tetrapods. *Nature* **513**:54-58.

Takeuchi M, Okabe M, Aizawa S. 2009. The genus Polypterus (bichirs): a fish group diverged at the stem of ray-finned fishes (Actinopterygii). Cold Spring Harbor Protocols 2009, 2009(5). pdb.emo117.

Tatsumi N, Kobayashi R, Yano T, Noda M, Fujimura K, Okada N, Okabe M, 2016. Molecular developmental mechanism in polypterid fish provides insight into the origin of vertebrate lungs. *Scientific Reports* **6**:30580.

Theveneau E, Mayor R. 2012. Neural crest delamination and migration: from epithelium-to-mesenchyme transition to collective cell migration. *Developmental Biology* **366**:34-54.

Tokita M, Schneider RA. 2009. Developmental Origins of Species-Specific Muscle Pattern. *Developmental Biology* **331**:311-325.

Walshe J, Mason I. 2003. Fgf signalling is required for formation of cartilage in the head. *Developmental Biology* **264**:522-536.

Warga RM, Nusslein-Volhard C. 1999. Origin and development of the zebrafish endoderm. *Development* **126**:827-838.

Willey A. 1891. The later larval development of amphioxus. *Quarterly journal of microscopical science* **32**:183-234.

Witzmann F. 2004. The external gills of Paleozoic amphibians. Neues Jahrbuch für Geologie und Paläontologie Abhandlungen **232**, 375-401.

Figure legends

Fig. 1: External gills of the Senegal bichir derive from the accelerated epidermal outgrowth of the hyoid segmental origin

(A) Budgett's illustration (Kerr 1907) of a 3 cm long bichir larva with prominent external gills (exg). (B) Lateral view of an early pharyngula stage, SEM image showing external gills and cement glands (asterisk) as the first forming cranial structures. (C) SEM image of an early neurula stage with emerging bulge within the hyoid domain (hd). (D) *Hoxa2* expression in the neural tube at the level of the presumptive hyoid arch. (E, G) SEM images of a tailbud embryo with external gills anlage. (F, H) *Hoxa2* expression pattern in a tailbud stage, with highlighted position of external gills. (I-L) SEM images showing developmental morphogenesis of external gills. (C-F, I-K) Dorsal view. (G-H, L) Lateral view. e, eye primordium; ot, otic vesicle; r3, rhombomere 3; r5, rhombomere 5.

Fig. 2: Accelerated formation and heterochronic development of the hyoid neural crest cells supply mesenchyme for the bichir external gills.

(A, D, G) *Sox9* expression pattern in NC cells, from neurulation until early tailbud stages, dorsal views. Notice that the population of hyoid NC cells (marks as H) forms very early, and it later represents the most prominent cranial NC stream. (B-C, E-F) *Sox9* expression pattern in the mandibular and the hyoid domain, respectively, transversal sections. White arrowheads mark the ventral position of the NC cells. Dotted lines represent boundaries of neural- (red) and non-neural (yellow) ectoderm. DAPI (blue) shows cell nuclei. (H) Pseudocolored SEM image, lateral view on an embryo with the partially removed surface ectoderm (blue). NC cells are green, notice the amount of hyoid NC cells. Mesodermal mesenchyme is reddish, endodermal pouches are yellow, and the neural tube is violet. (I-K) Sox9 antibody visualizes individual neural crest cells. Lateral views, with small insets representing dorsal views. Black arrowheads in I show the advanced position of the hyoid NC cells. (L-O) Hyoid NC cell fate mapping (DiI red). Superimposed fluorescent and dark-field images at successive stages of development. (L) Lateral view, stage 25 embryo showing the hyoid NC stream. Small inset (dorsal view) represents an embryo at stage 20 immediately after the focal DiI injection into the rhombomere 4 (r4). (M-N) DiI signal at developing external gills, dorsal views. (O) Transversal section through the external gill (exg) at the level indicated in O. White arrow shows DiI signal in the primary branch of the external gill. Asterisk, cement gland; e, eye primordium; H, hyoid NC stream; Ma, mandibular NC stream; np, neural plate; ot, otic vesicle; r3, rhombomere 3; r4, rhombomere 4.

Fig. 3: The premature differentiation of the external gill-associated cranial muscle complex in the Senegal bichir larva

(A-C) Dorsal view on bichir embryos, developing skeletal muscles are revealed by 12/101 antibody (red). The red signal in A (st. 27) refers to the post-otic somites. The first cranial muscle is associated with the external gills (B, stage 29). (C) Superimposed fluorescent and SEM image showing the context of the external gill muscles. (D) Transversal section through the external gills at the level indicated in B. DAPI (blue) stains cell nuclei. (E, F) Stage 30 bichir embryo, lateral view with (E) cranial nerves fibres labeled with anti-acetylated tubulin, and with (F) cranial muscles stained with 12/101 antibody (red). (G) Stage 33 bichir embryo, lateral view, with developed cranial muscles stained with 12/101 antibody (red). Asterisk, cement gland; am, adductor mandibulae; ah/ao, complex of adductor hyomandibulae and adductor operculi; b, brain; ba, branchial arches; bm, branchiomandibularis; cd,constrictor dorsalis; cement gland; e, eye primordium; lb/db, complex of levator branchiarum and depressor branchiarum; hh, hyohyoideus; ih, interhyoideus; im, intermandibularis; ot, otic vesicle; pf, pectoral fin; y, yolk; V., nervus trigeminus; VII., nervus facialis.

Fig. 4: Considerable expansion of the hyoid pharyngeal endoderm contributes to the development of external gills in the Senegal bichir.

(A, F) SEM images, dorsal view of bichir embryos with developing external gills (exg), showing the level of virtual sections in B and G. Notice the correspondence of the hyoid pharyngeal endoderm (B, G) and the external gills (A, F). (B-D, G-H) 3D models of pharyngeal endoderm (yellow) from dorsal (C, H), and lateral (D, I) view, respectively. (E, J) Transversal sections show prominent lateral expansion of hyoid pharyngeal endoderm (white arrow). (K-M) Transversal sections show wild-type expression of *Fgf8*, *Pea3*, and *Dusp6* (black arrow) in the external gills primordium. (N) Immunostaining of anti-activated MAP kinase antibody on transversal section of the external gills primordium. (O) Scheme summarizing *Fgf8*, *Dusp6*, and *Pea3* (K-M) expression patterns in the external gills formation at stage 26. Violet indicates *Fgf8* expression; blue marks *Dusp6* expression in the endoderm and adjacent mesenchyme of the external gills; yellow depicts expression of *Pea3* in the mesechyme of the external gills. (P-U) Inhibition of pouch-like endodermal outpocketings (P, R, T-U), dorsal view. (P-Q) Control larvae treated with DMSO develop normal pouch-like endodermal outgrowths (white arrow). (R) Larvae exposed to SU5402 from stage 20 till stage 26. (S) Transversal section shows loss of external gill anlagen. (T-U) SU5402 treated larvae fixed at stage 26 and probed for *Pea3* (T) and *Dusp6* (U). Nuclei are stained with DAPI (blue), basal laminae with anti-fibronectin (red). White arrowheads mark spiraculum (hyomandibular cleft) and black arrowhead marks hyo-branchial pouch. Asterisk, cement gland; b, brain; green, otic vesicle; e, eye primordium; nt, notochord; ot, otic vesicle; ph, pharynx.

Fig. 5: Bichir embryos diverge from the common anteroposterior differentiation scheme by accelerated development of the entire hyoid segment.
(A, B) A cartoon of cranial neural crest migration (green), the first mesoderm (red), and pharyngeal pouches (yellow) in a typical vertebrate (A) and a bichir (B). Top are left lateral views, below are left horizontal sections. (A) In vertebrates, the sequential anteroposterior formation of cranial segments is well conserved, including pharyngeal pouches and cranial neural crest streams. (B) In bichirs, the entire hyoid segment is accelerated with earlier formation of the endodermal, mesodermal, and neural crest tissues, what constitutes a developmental basis for the appearance their external gills. Surface ectoderm in horizontal sections is shown in blue and primitive gut in ochre; B, branchial NC stream; H, hyoid NC stream; Ma, mandibular NC stream; pp I.-pp VI., pharyngeal pouches.

Fig. 4-figure supplement 1: Fgf8 expression during the course of bichir hyoid arch and external gill development. (A-J) *Fgf8* expression patterns at the indicated stages from dorsal (A-E), and lateral (F-J) views, respectively. (K-O) Sections at the level of the external gills (exg). White arrowheads mark spiraculum (hyomandibular cleft) and black arrowheads mark hyo-branchial pouch. White arrow indicates presence of *Fgf8* transcripts in the hyoid endodermal outpocketings. Asterisk, cement gland; b, brain; nt, notochord; ph, pharynx.

Fig. 4-figure supplement 2: Expression patterns of bichir* Fgf8 *and transcriptional readouts of Fgf signaling,* Dusp6 *and* Pea3*. (A, D, G, J) *Fgf8* expression patterns at the indicated stages from dorsal (A, G), and lateral (D, J) views, respectively. (B, E, H, K) *Dusp6* expression patterns at the indicated stages from dorsal (A, G), and lateral (D, J) views, respectively. (C, F, I, L) *Pea3* expression patterns at the indicated stages from dorsal (A, G), and lateral (D, J) views, respectively. Asterisk, cement gland; exg, external gills.

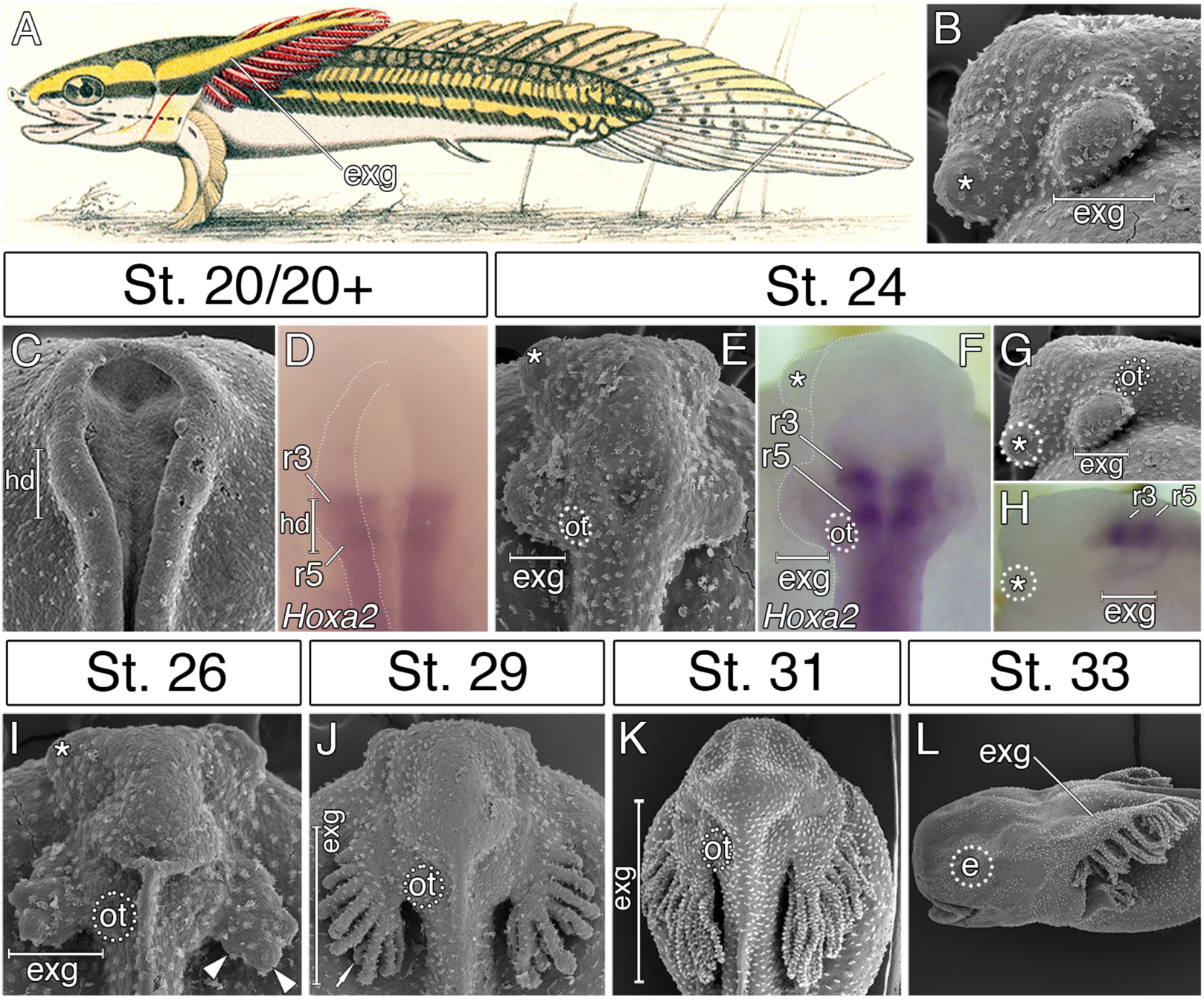
A
exg
B
*
exg
St. 20/20+
St. 24
C
hd
D
r3
hd
r5
Hoxa2
E
*
ot
exg
F
*
r3
r5
ot
exg
Hoxa2
G
ot
*
exg
H
r3
r5
*
exg
St. 26
St. 29
St. 31
St. 33
I
*
ot
exg
J
exg
ot
K
ot
exg
L
exg
e

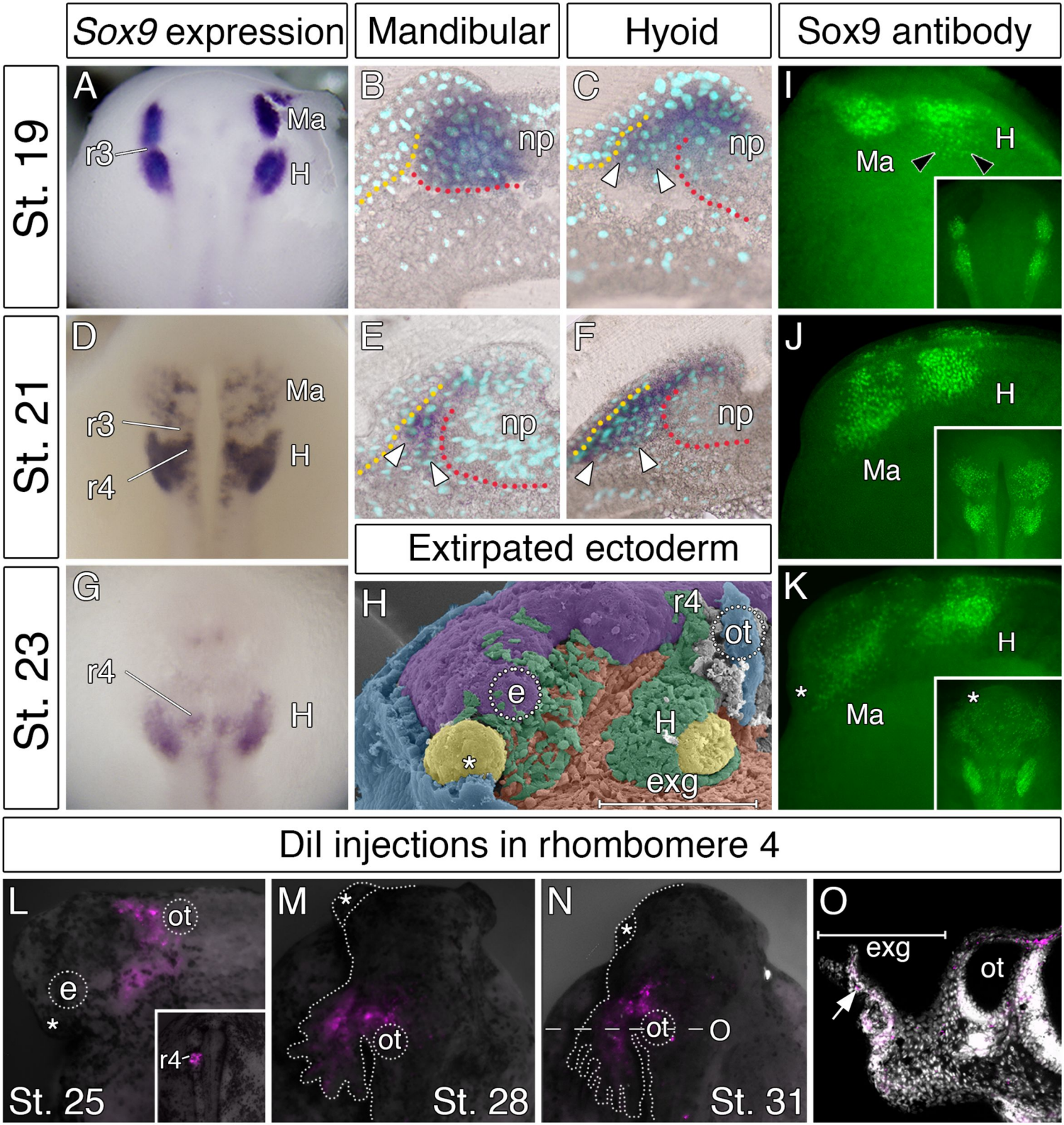
Sox9 expression
Mandibular
Hyoid
Sox9 antibody
St. 19
St. 21
St. 23
A
Ma
r3
H
B
np
C
np
I
H
Ma
D
Ma
r3
r4
H
E
np
F
np
J
H
Ma
Extirpated ectoderm
G
r4
H
H
r4
ot
e
*
H
exg
K
H
*
Ma
*
Dil injections in rhombomere 4
L
ot
e
*
r4
St. 25
M
*
ot
St. 28
N
*
ot
O
St. 31
O
exg
ot

St. 27
A
*
e
ot
St. 29
B
e
ot
D
C
e
ot
D
exg
ot
b
ba
y
St. 30
E
VII.
e
V.
exg
*
F
e
exg
*
St. 33
G
ah/ao
lb
cd
e
db
-am
pf
bm
im
ih
hh

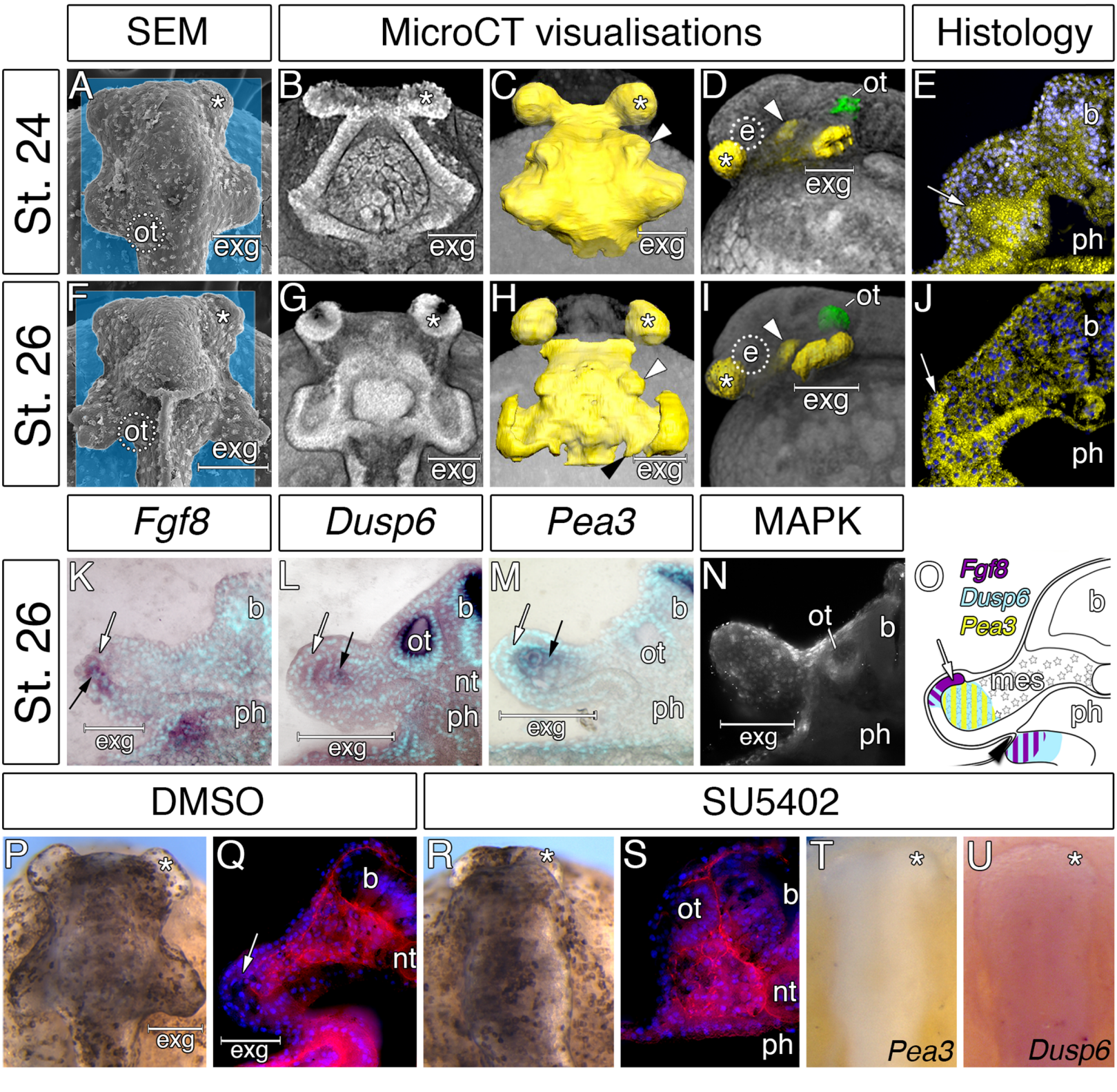
SEM
MicroCT visualisations
Histology
St. 24
St. 26
A
B
C
D
E
F
G
H
I
J
ot
exg
e
b
ph
Fgf8
Dusp6
Pea3
MAPK
K
L
M
N
O
nt
mes
DMSO
SU5402
P
Q
R
S
T
U

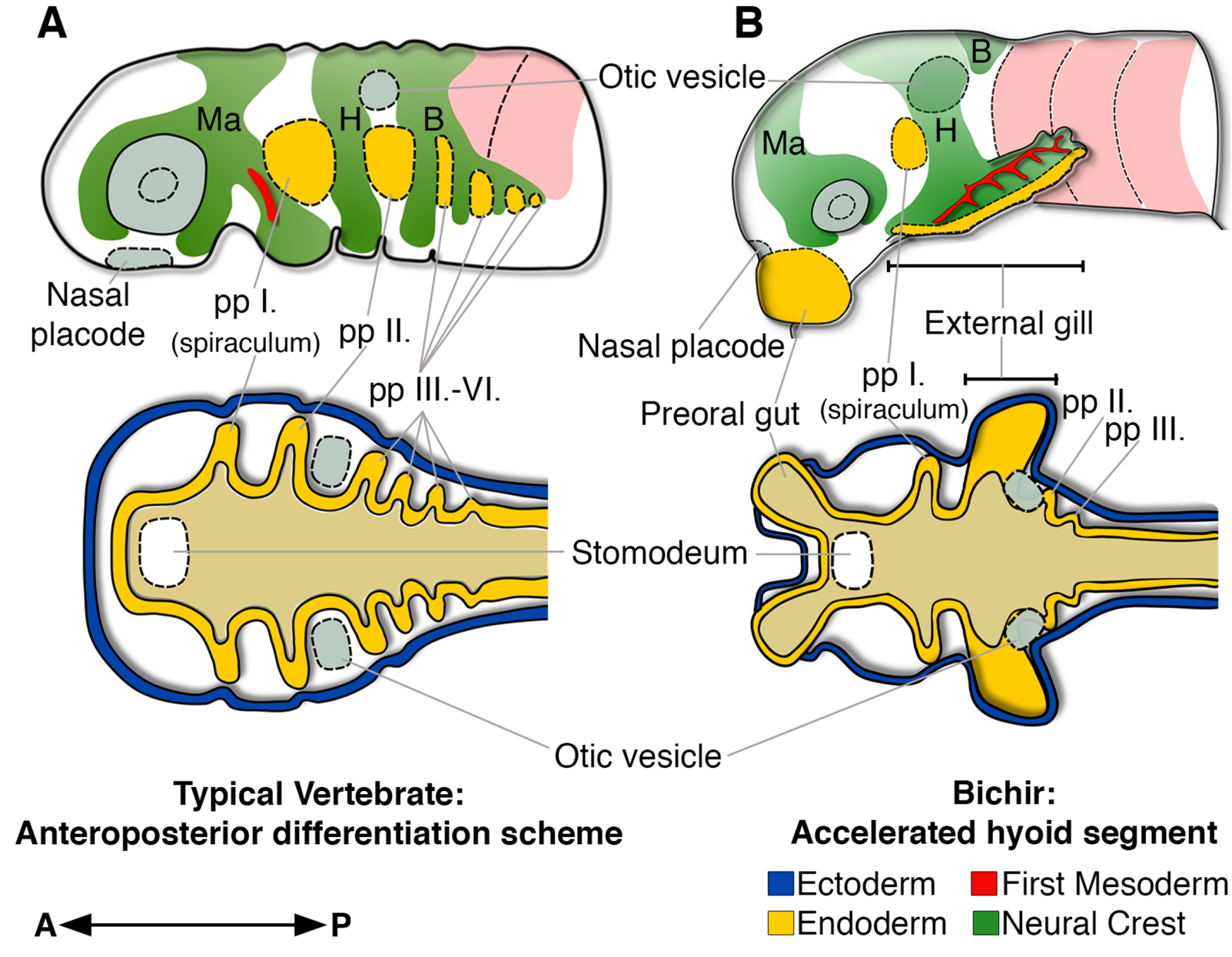
A
Ma
H
B
Otic vesicle
Nasal placode
pp I. (spiraculum)
pp II.
pp III.-VI.
Stomodeum
Otic vesicle
B
Ma
H
B
Otic vesicle
Nasal placode
External gill
Preoral gut
pp I. (spiraculum)
pp II.
pp III.
Typical Vertebrate:
Anteroposterior differentiation scheme
A
P
Bichir:
Accelerated hyoid segment
Ectoderm
First Mesoderm
Endoderm
Neural Crest

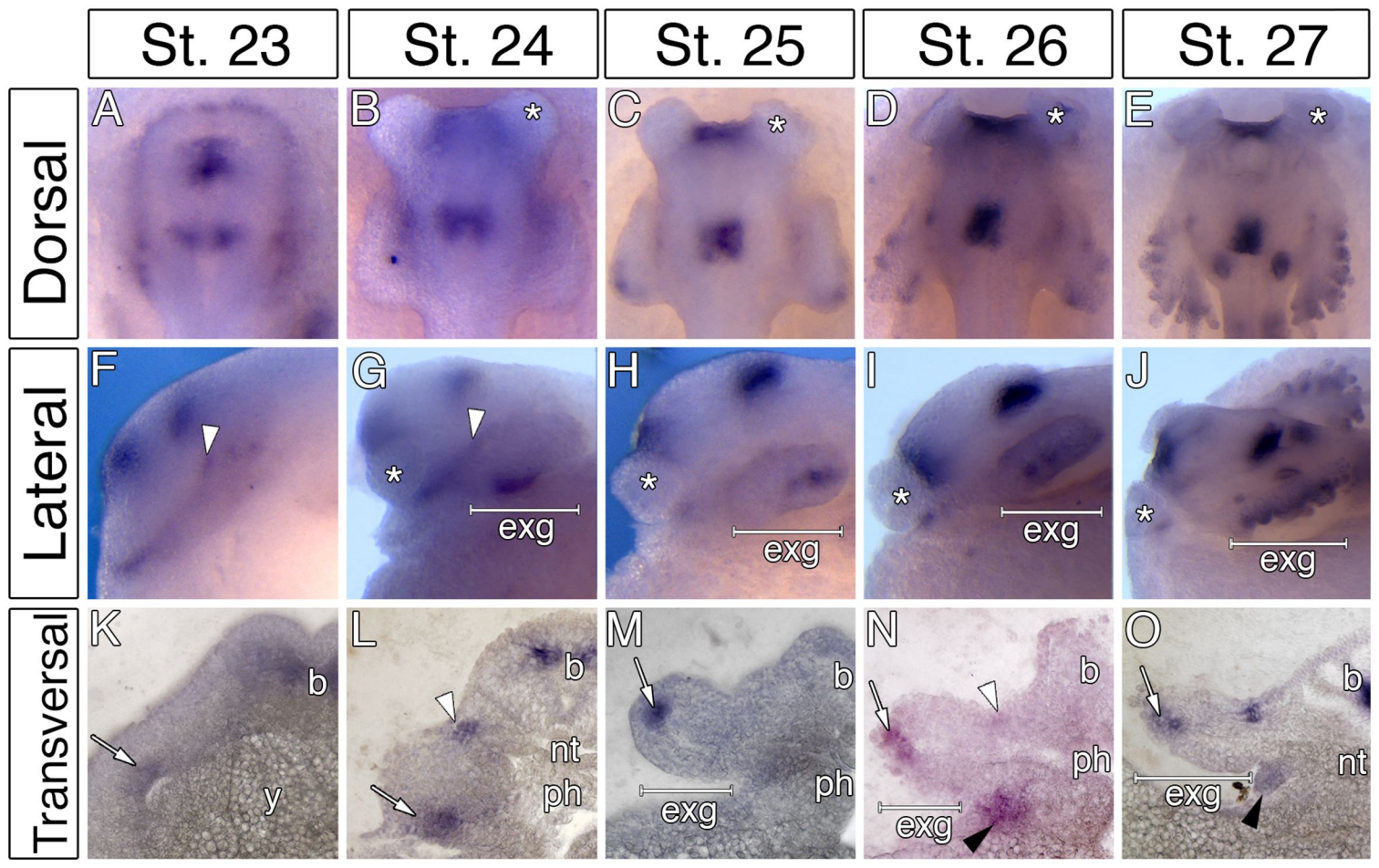
St. 23
St. 24
St. 25
St. 26
St. 27
Dorsal
Lateral
Transversal
A
B
C
D
E
F
G
H
I
J
K
L
M
N
O
*
exg
b
y
nt
ph

Fgf8
Dusp6
Pea3
st. 24
st. 26
Dorsal
Lateral
A
B
C
D
E
F
G
H
I
J
K
L
exg